

An Optimal DC Microgrid for Hybrid Consumer Loads and Electric Vehicle Integration

Raghumanth A^{1*} and Rex Joseph²

¹Research Scholar, EEE Department, PES University, Bangalore, Karnataka, India - 560085; raghumantha@pesu.pes.edu

²Professor, EEE Department, PES University, Bangalore, Karnataka, India – 560085

*Correspondence: Raghumanth A; raghumantha@pesu.pes.edu

ABSTRACT- Increasing use of electrical energy at domestic consumer level due to increased usage of electrical appliances, compounded with increased electric vehicle usage will cause severe stress on existing distribution networks necessitating expensive infrastructural changes. An alternative would be to increase consumer level energy production through renewable sources so that dependence on the grid is eliminated altogether, or minimized. This would also help reduce overall carbon footprint. This paper discusses a viable implementation of a DC micro-grid with battery storage that is compatible with the majority of existing loads and also suggests modifications in certain loads to make them compatible. The micro-grid also allows for DC charging of electric vehicles at different voltage levels. The compatibility with the proposed Microgrid, of loads that can function without modifications and those that require minor changes is analyzed and verified experimentally.

Keywords: Battery charging, BESS, BMS, DC - DC converter, Electric Vehicle, Hybrid Electrical Loads (HEL), Renewable sources.

ARTICLE INFORMATION

Author(s): Raghumanth A and Rex Joseph;

Received: 24/07/2024; **Accepted:** 01/10/2024; **Published:** 15/10/2024;

e-ISSN: 2347-470X;

Paper Id: IJEER 2407-29;

Citation: 10.37391/ijeer.120402

Webpage-link:

<https://ijeer.forexjournal.co.in/archive/volume-12/ijeer-120402.html>



Publisher's Note: FOREX Publication stays neutral with regard to Jurisdictional claims in Published maps and institutional affiliations.

1. INTRODUCTION

With the need to reduce dependence on fossil fuels due to their detrimental effects on the environment, the usage of renewable energy has gained importance [1] – [3]. Traditionally renewable energy has for most part been integrated into the existing grid at source level [4]. This is true even in cases where the source is DC, like solar photo-voltaic systems [5]. This is because of the structure of the conventional grid, and the end use loads being AC loads [6]. The drawback of following this model is that increasing energy demands would need revamping of the transmission and distribution network which will be stressed beyond designed capacity [5].

This is the model that is adopted in rooftop solar generation, which needs to be increased to meet the local demand [7], [8]. The model for consumer level generation is to convert the generated voltage to grid level AC and supply that to the residential loads, and any excess will be purchased by the utility. However solar energy which is inherently DC, needs to be converted to AC before supplying to the grid or local loads [9], [10]. This conversion will lead to lower efficiency, and can be avoided due to the shift of loads to DC or hybrid ones which

are power converter fed [5], [6]. In this paper, hybrid loads refer to those that can operate with similar performance on both AC and DC supplies without modifications or the need for additional power converters. A class of these loads have conversion to DC as an intermediate step even if the source is AC [5], [11], [12]. The need for bolstering distribution network can be avoided if consumer level distributed generation (DG's) from renewable sources is increased [13].

Modern loads can be broadly grouped into those capable of being also operated of a DC supply, those that need minor changes to enable DC operation, and those that require an additional converter for DC operation [5], [14], [15]. If all loads are DC supply compatible, then, coupled with battery energy storage systems, reliable and efficient operation of all consumer loads can be ensured [16], [17]. Having storage also allows for reduction of peak demands on the utility, since energy management can be done, and this can be extended to charging of electric vehicles, which is another load that is expected to increase rapidly and have charging periods coincident with existing peak demand [18], [19], [20].

Due to the advent of electric vehicles, battery technology is expected to evolve and other economical and reliable storage option, and this can be leveraged in a DC system [21]. Present system consists of a BESS and an inverter, this further reduces the reliability of the system [5]. If only BESS is used as source as proposed reliability is higher as compared to an Inverter system[5]. Ongoing research in other storage options like super-capacitors and fuel cells are expected to improve their characteristics, and they too are DC sources. Having local storage prevents energy being un-utilized in the event of grid outage and also ensures continued supply, a role that is currently

being performed by uninterruptible power supplies with battery storage [22], [23].

This paper discusses the implementation of a DC grid for various types of electrical loads and proposes an optimal DC voltage level that can be adopted to minimize changes to existing consumer electrical devices. These electrical loads, which can operate on both AC and DC, are termed Hybrid Electrical Loads (HEL). The proposed voltage levels have been less explored, as the most common scenario involves designing loads for typical 48 V systems [24], [25]. The proposed grid system is a complete DC source that can be extended to smaller distribution networks to form a micro-grid, allowing for local energy exchange and a more stable demand-supply balance. This energy interchange is easier in a DC system since synchronization issues like frequency and phase difference are not required. The DC bus is formed using a Battery Energy Storage System (BESS) charged from a solar photovoltaic source. The paper also proposes and demonstrates modifications needed for some electrical loads to be compatible with a DC source. These changes can be mandated by standards to enable all loads to be hybrid, capable of operating on both AC and DC sources. This transition to a DC system would incur lower expenses, increase efficiency, and enhance reliability [5]. The paper is structured as follows: Section 2 classifies electrical loads, Section 4 defines DC link voltage levels, Sections 5 and 6 present simulation and hardware results, and Sections 6 and 7 provide results, discussion, and conclusions.

2. CLASSIFICATION OF ELECTRICAL LOADS

2.1 Appliances that require no modification to be able to operate with both AC and DC sources –HEL

2.1.1 Loads with active front end converter

Many domestic appliances have a power factor correction (PFC) stage, an intermediate DC link and a DC-DC power converter. Examples include inverter based - washing machines, air conditioners, microwave ovens and refrigerators that have a variable speed drive or high frequency circuits for efficient operation. These devices often include a high-frequency self-starting converter for auxiliary control voltage. Since both the PFC front-end converter and auxiliary supply can operate with AC or DC, no modification is needed for DC operation within a specified voltage range. Such loads are termed as HEL in this paper. *Figure 1* and *figure 2* shows the typical block diagram of above-mentioned electrical loads.

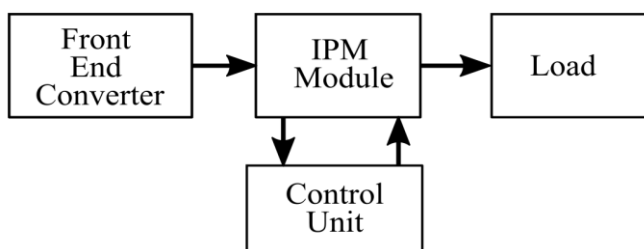


Figure 1. Block diagram of Inverter based washing machine and AC

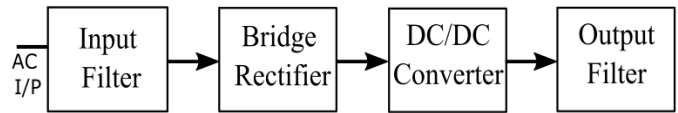


Figure 2. Typical block diagram of modem-day adapters.

2.1.2. Loads with universal motor: Certain domestic appliances like food processors and power tools use a series motor. Although these are tailored to work on AC, the motor is a universal motor, and so can be operated on a suitable DC voltage level also [5]. While the absence of inductive reactance would cause some change in operating point, the type of applications is not those that would be affected adversely.

2.2 Appliances requiring minor modifications in order to convert them as HEL

Some of the Electrical appliances that require few minor modifications such that direct DC can be applied is discussed in the following sub sections.

2.2.1 Loads with low frequency transformer for auxiliary supply: It is observed that there are some loads that use a low frequency transformer and linear power supply IC's to power up the internal control circuitry as shown in *figure 3*. This linear power supply needs to be replaced with a low power self oscillating flyback converter. This can be mandated by regulations for compliance so that these loads are also DC compatible.

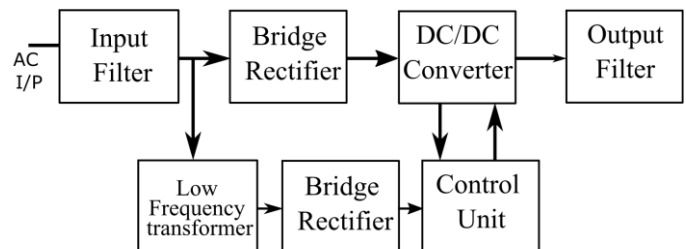


Figure 3. Typical Block diagram of applications with low frequency transformer

2.2.2 Electrical Appliances with thermostat switch: Many heating loads like the electric iron and water heaters use a thermostat to switch ON and OFF the supply to the heating element employing a simple mechanical hysteresis control. In those loads, when with DC source, it was observed that thermostat switch does not break the circuit when the upper temperature has reached [5]. The non-existence of zero crossing as in the case of AC source caused an arc to form between the contacts keeping the circuit closed and causing the temperature to rise further. This particular issue has been addressed in the paper.

2.3 Appliances that need an additional converter in order to convert them as HEL

Induction motors are widely used in domestic appliances like fans, blowers and pumps for example. Since most of these use either no speed control, or use elementary stator voltage control, they do not use any power converter, and are as such

incompatible with DC input. Single phase induction motors have low efficiency and to overcome this, brushless DC motors are being used. The BLDC motor based loads are compatible with DC supply, but the induction motors would require a power converter to facilitate DC operation. This will have the advantage of higher efficiency, and additional control using Internet of Things (IoT) or being WiFi enabled can make the user experience better. However, this class of loads is considered incompatible in this paper.

3. POWER LOSS CALCULATION WITH AC AND DC INPUT TO A PFC STAGE FRONT END CONVERTER

In this section, the power losses are computed for either AC or DC input to validate the satisfactory operation on DC. The losses are computed for the power switches, diode and inductor to show that the overall losses are similar in either case, and the same has been experimentally verified by measuring the temperature rise. The computations are done as per [12], [13].

3.1 MOSFET Conduction Losses

Losses of some of the major components.

$$I_{Q-rms} = \frac{I_{PK}}{2\sqrt{\pi}V_o} \sqrt{2\pi V_o^2 - 4V_{PK}V_o + \pi V_{PK}^2} \quad (1)$$

$$P_Q = r_{DS-on} * I_{Q-rms}^2 \quad (2)$$

For an AC input of 230 V, as per 3.1 following solution is obtained,

$$I_{Q-rms} = 1.028 * I_{PK} \quad (3)$$

For an DC input of 220 V, as per 3.1 following solution is obtained,

$$I_{Q-rms} = 0.633 * I_{PK} \quad (4)$$

When we compare *equation 3*, *equation 4* conduction losses of the switch are reduced when the converter is powered from DC input.

4. DESIGN OF PROPOSED DC GRID COMPONENTS

4.1 Design and selection of system components

- EV scooters/two-wheeler which are being used to commute to workplace is on the rise which in turn increases the load on the existing system. Establishing a charging station at work place is very essential to avoid such loading on the grid during peak hours.
- To achieve this, use of renewable energy resources is needed and worthwhile since emissions due to fossil fuel burning can be reduced.
- In this section we talk about different components that has been designed and selected for the setup of charge station

locally based on solar DC micro grid. Typical block diagram of the proposed system is as shown in *figure 4*.

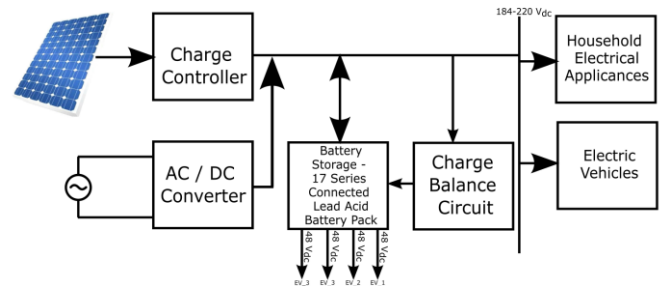


Figure 4. Proposed Block Diagram

4.2 Solar panels

Solar modules of 250 W each - that can generate on an average of 5 kWhr per day and has an open circuit voltage of 36 V and short circuit current of 6.9 A. It is connected in series which boosts the open circuit voltage to 144 V.

4.3 Battery Energy storage system (BESS). In the proposed system, *table 1* provides the specifications parameters used as BESS.

Table 1. Battery parameters used in the system

Parameters	Specifications (Nominal)
Voltage (Each battery)	12 V
Capacity	42 Ah
Technology	SMF Lead acid
Number batteries used (Series)	17

4.4 Charge circuit

A SEPIC converter which can step up or down based on the input voltage is used for charging the BESS. 4 panels, each of 36 Voc are connected in series as input to the converter.

4.4.1 Design of Charge circuit

The charge circuit uses a SEPIC converter for flexible voltage regulation. A bulk capacitor at the input stores energy and stabilizes the input supply. *Table 2* presents the design specifications, and *table 3* shows the calculations for selecting the required components.

The SEPIC converter operates by transferring energy through two inductors and a capacitor, allowing it to efficiently convert a wide range of input voltages into a stable output. The circuit is designed to maintain Continuous Conduction Mode (CCM), where the current through the inductors never falls to zero, ensuring smooth and consistent operation. The key advantage of using a SEPIC converter is its ability to maintain output regulation regardless of input fluctuations, making it ideal for solar-based systems where input voltage can vary throughout the day.

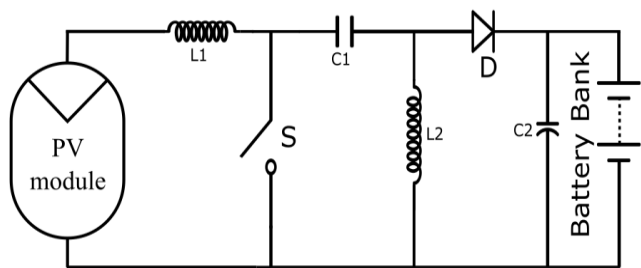


Figure 5. Illustrates the SEPIC converter design

Table 2. DC Grid Specification

Sl. No.	Parameters	Specifications (Nominal)
1	Input Voltage (From Series connected PV)	100 V - 150 V
2	Output Voltage (Battery Pack Voltage)	185 V - 230 V
3	Charging current	5 A
4	Total output power	1 kW

Table 3. Components selected based on the specifications

Sl. No.	Selection Criteria	Component
1	Maximum Voltage and current stress on the switch is given by $V_{in} + V_o$ (Max condition) = $144 + 230 = 375$ V	IRFP460
2	Output diode: Maximum reverse voltage, $V_{rms} = V_{in} (max) + V_o(max)$ and output rms current is 5 A	MUR860
3	Inductor selection (L1 and L2)	1 mH

4.5 Proposed Charge balance circuit

Since the cell chemistry used is lead acid, charge balancing is normally not required. However, the option of varying voltage taps for different voltage levels at the load would lead to unbalance that needs to be compensated. The balancing is required even with no taps at different voltages, if other sensitive chemistries were used, like lithium for example. Flyback topology is used for balancing the batteries. The system generates four 48 V buses for electric scooter or bicycle charging, and a 220 V bus for household appliances.

5. EXPERIMENT AND RESULTS

5.1 Simulation of Charge Circuit

Matlab/Simulink platform is used to understand the behavior of the charge controller. Figure 6 shows the simulated charge circuit with P and O algorithm for maximum power point tracking on the solar panel input. The Simulation is carried out for the DC grid voltage levels proposed and which has been set up in the lab. Figure 7 and figure 8 are the simulation results of

the SEPIC charge controller, displaying the output voltage and state of charge during charging with respect to time.

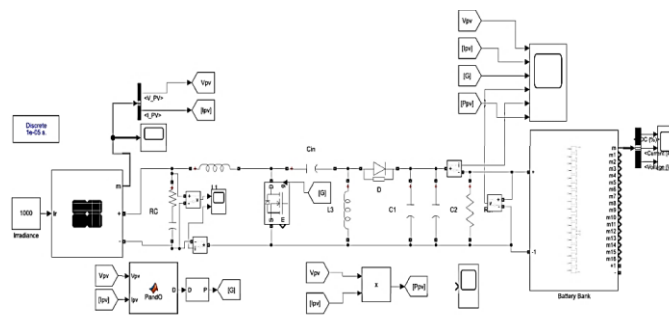


Figure 6. SEPIC_Charge circuit

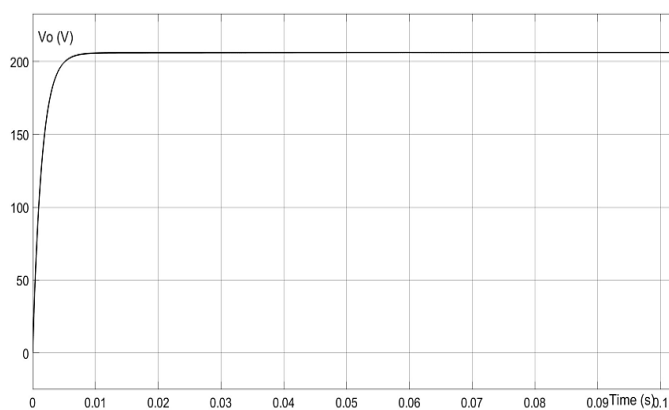


Figure 7. Vo During Charging

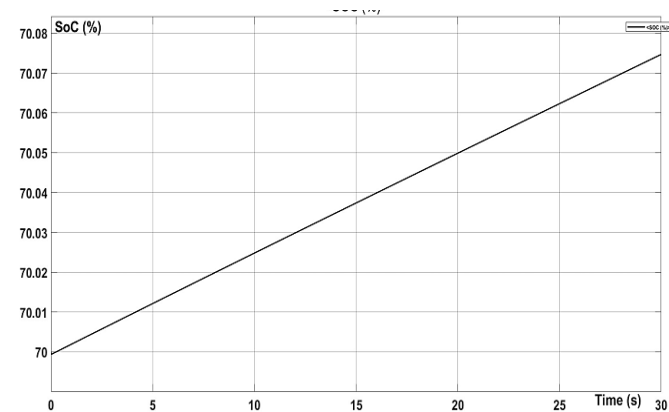


Figure 8. SoC during charging

5.2 Simulation of Charge Balance Circuit

Figure 9 shows the topology (Fly-back) used for charge balance circuit. There are three subsystem blocks:

- Multi winding transformer section has a single primary with 17 secondary winding.
- Output Rectifier Section has 17 sets of half wave rectifier with filter capacitor.
- Battery Section comprises of 17 lead acid battery profile connected in series.

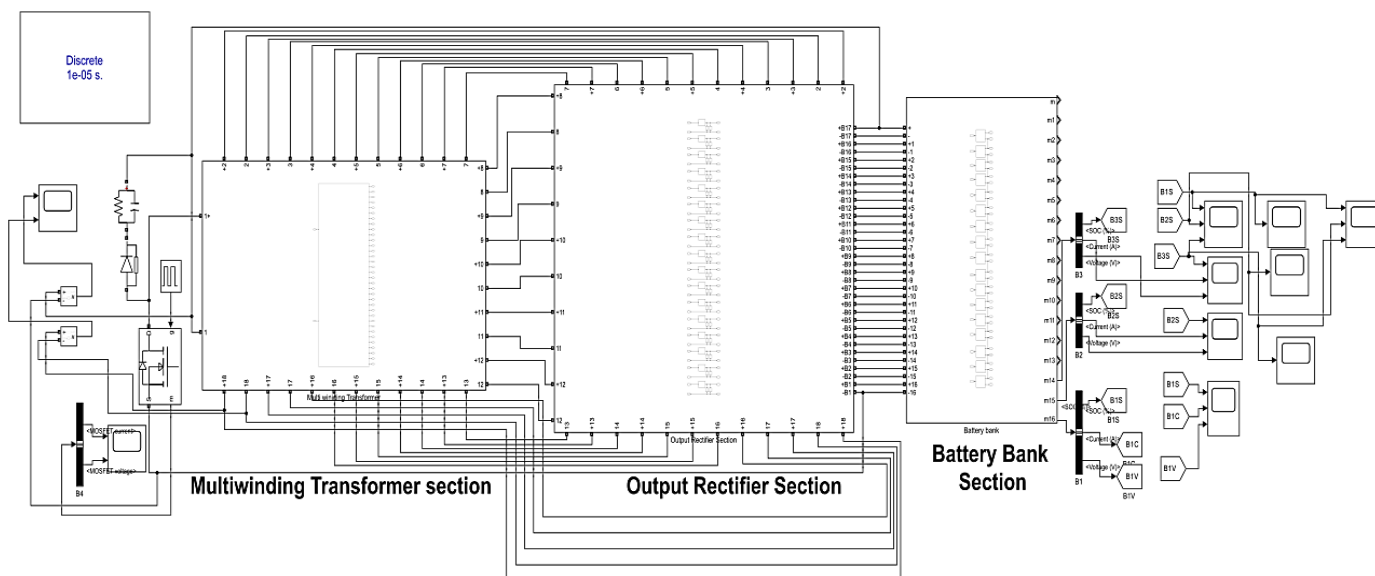


Figure 9. Simulation Circuit for charge balance

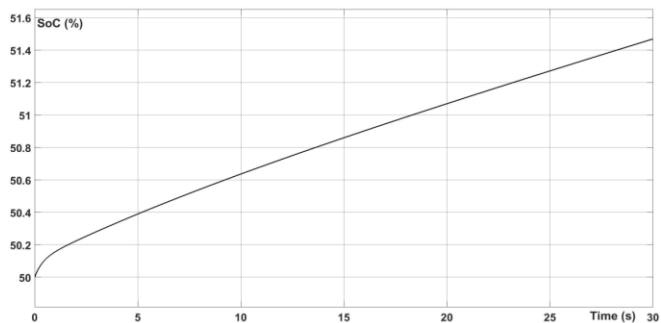


Figure 10. SoC of battery B1

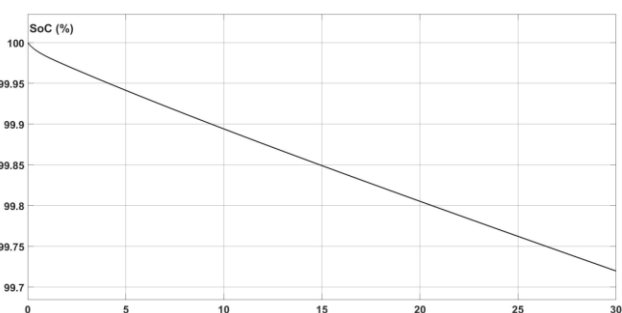


Figure 11. SoC of Battery B2

Figure 10 and figure 11 shows SoC (state of charge) of the battery B1 (Bottom most of the battery pack), SoC of battery B2 respectively. For test conditions, SoC of rest of the battery is kept at 100% as compared to the bottom most battery which is kept at 50%. As can be seen from the results over a set period of simulation time that the SoC of the battery B1 increases and the SoC of other battery B2 decreases indicating that the energy from the charged battery is transferred to the battery with lower SoC (B1).

5.3 Hardware results of Solar charge controller with active balancing unit

The charge from solar to the battery is controlled by a 1 kW SEPIC converter (Figure 12), designed with two inductors. The gate drive circuit, powered by the auxiliary supply, is optimized using TLP152. Since proposed DC grid as discussed in section 4 has multiple tapings in the BESS to achieve 48 V system. This results in mismatch of SoC – state of charge in individual battery units. In this DC grid active cell/battery balancing has been implemented using flyback topology whose primary input is the entire battery stack voltage. Figure 14 and figure 15 represents the drain to source voltage and output voltage of the SEPIC converter respectively. It can be observed that SEPIC converter is operating in CCM due to large inductance value which is used to smoothen out the output current. Figure 13 represents the charge balance circuit with UU100 core. Figure 16 is the scope waveform of Vds, Ids across the switch of the flyback topology and figure 17 represents the Vo and Io of the bottom most battery.

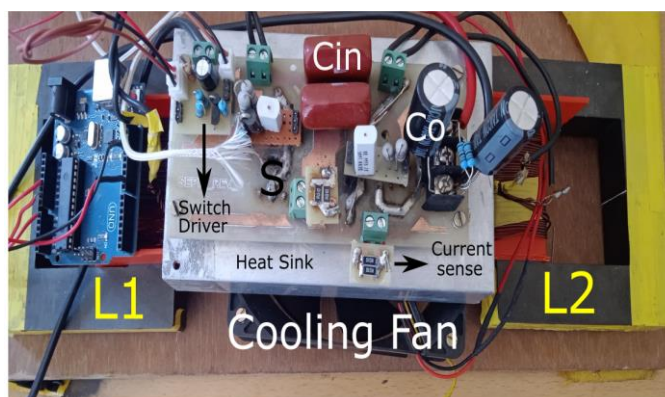


Figure 12. Charge Circuit

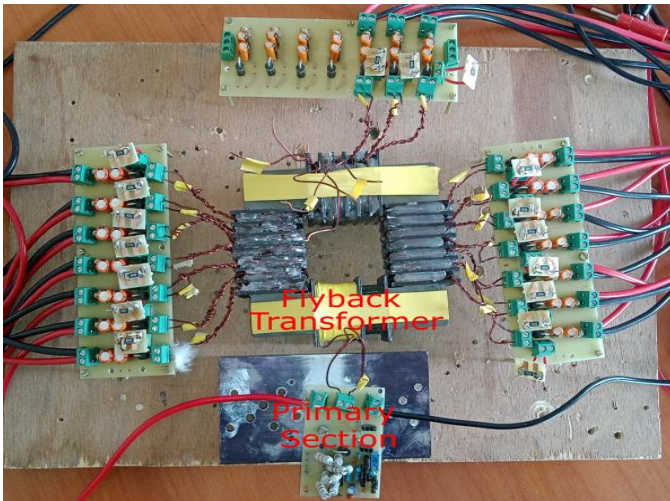


Figure 13. Charge Balance circuit

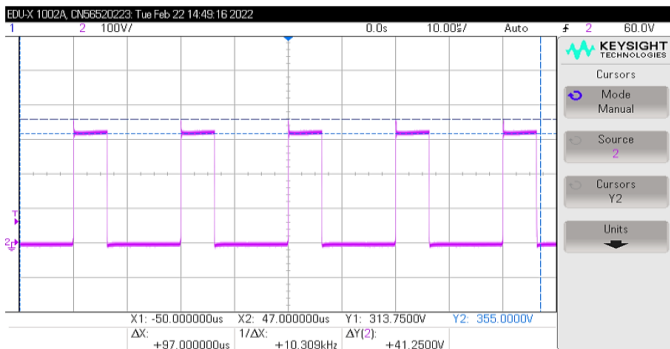


Figure 14. Vds_SEPIC_Converter

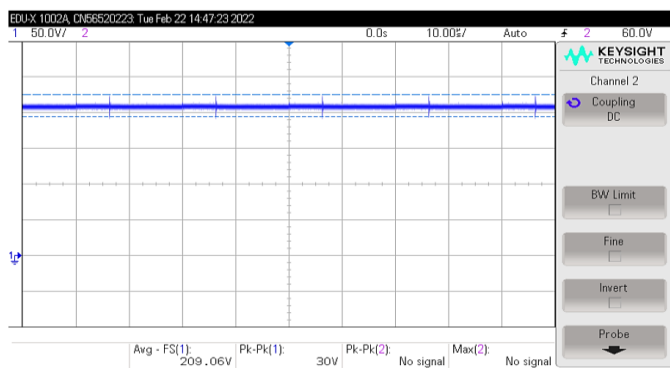


Figure 15. Vo_SEPIC_Converter

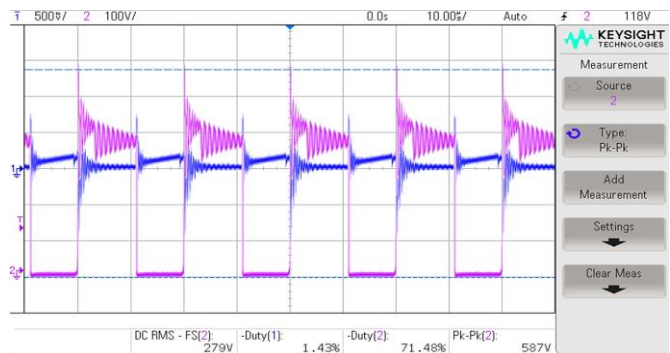


Figure 16. Vds, Ids_Battery Balancing Circuit

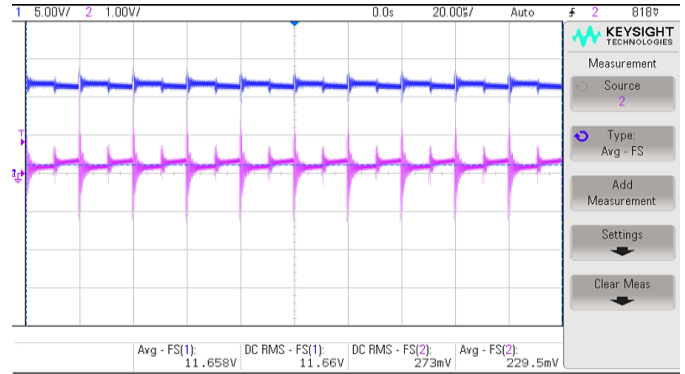


Figure 17. Vo, Io of Bottom most battery

5.4 Temperature rise in Power switch (IGBT) of Induction Stove

In this test, Induction stove is supplied with varying AC and DC voltages. J type thermocouple is placed on the body of the IGBT and continuously monitored. It can be observed that from figure 18, temperature of the switch (Y-Axis) (IGBT) is within nominal values if the DC voltage is maintained within the RMS of AC voltage.

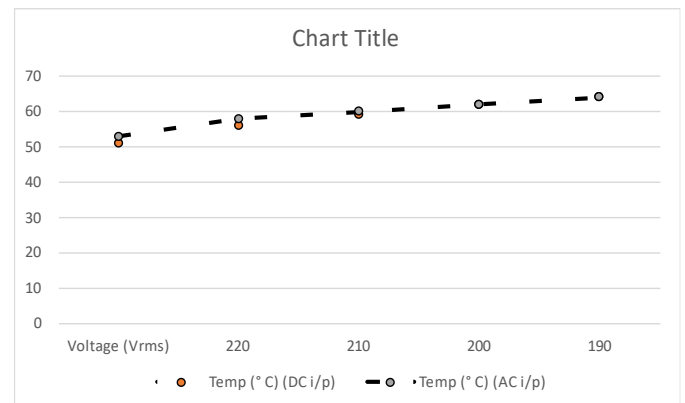


Figure 18. Temperature rise in power switch with AC and DC input.

6. MODIFICATIONS TO SOME OF THE CONSUMER LOADS

6.1 Iron Box/thermostat switch based loads

It is observed that during an interruption of the switch when supplied from DC grid, the two terminals of thermostat switch ended up getting welded together. This was because there is no zero crossing of load current, and the thermostat designed for AC operation could not interrupt the DC current. This lead to increased contact temperature and ultimately welding of the contacts. In order to eliminate this, capacitor was added across the contacts to ensure a bypass for current when the contacts open. This would extinguish the arc as fast as possible and the results were satisfactory. There was consistent extinction of the arc and breaking of circuit, leading to satisfactory performance. However, the capacitor would result in a path for small AC current flow even with the contacts open.

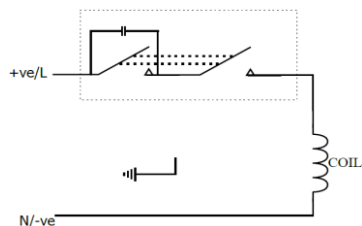


Figure 19. Iron Box Modification suggested for use with both AC and DC input

Figure 19 shows the modification to be done on the existing Iron box and it is suggested to have two ganged contact points connected in series, with the capacitor across one of them. This would ensure that the thermostat works efficiently for both AC and DC input making them HEL. Figure 20 illustrates the current through the thermostat switch in an iron box, without the external capacitor, when the input supply is a DC source. The current is measured across the 0.1Ω shunt resistor. Initially, at time t_1 , the thermostat switch is ON. As the desired temperature is reached, the switch attempts to turn OFF at time t_2 . However, the current does not drop to zero which can be observed between t_2 and t_3 and continues to arc between the terminals, as shown in figure 22. To avoid permanent damage to the thermostat, switch an external switch is operated manually to interrupt the current at t_3 . Figure 21 shows the current waveform with $2.2 \mu\text{F}$ capacitor across the switch and as can be seen, it clearly interrupts the current. The same phenomenon can be validated from figure 23 as well.

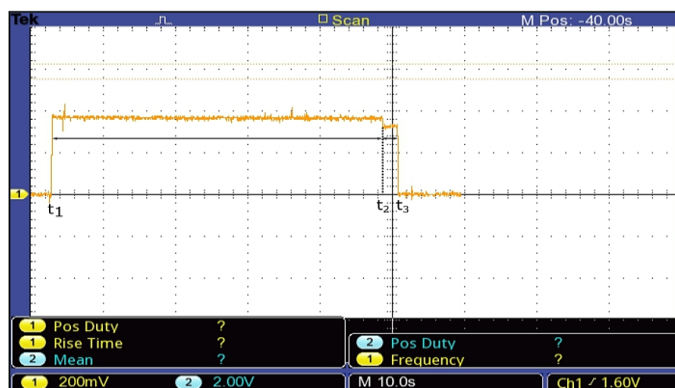


Figure 20. Current through Iron Box/Thermostat Switch without capacitor

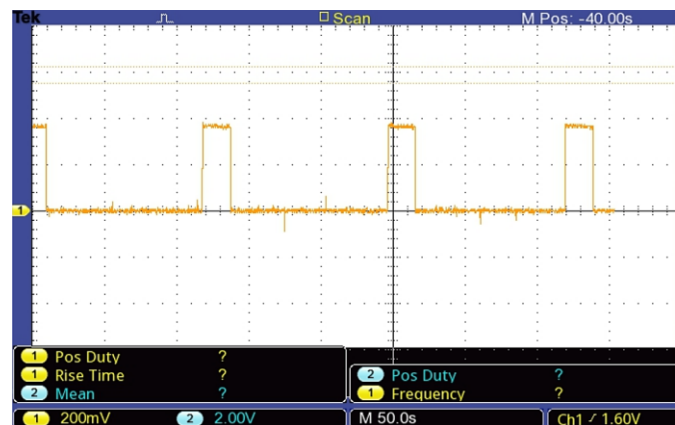


Figure 21. Current through Iron Box/Thermostat Switch with $2.2 \mu\text{F}$



Figure 22. Arcing across the switch without capacitor



Figure 23. Arcing across the switch with capacitor

6.2 Induction motor Loads

Single phase induction motors are widely used in fans and pumps in domestic applications. Single phase motor loads have been successfully operated on DC with a two-phase inverter for energizing the coils, and this can be adapted, with a front end rectifier, for use on both AC and DC. While this would add to the initial cost, the improved efficiency would lead to lower operating costs. Having an inverter would also enable wireless control and compatibility with IoT protocols can be ensured. This would enable, for example programming of speeds based on user comfort levels, leading to a better usage experience as an added advantage.

6.3 Low frequency transformers

In loads which are otherwise compatible but use a low frequency transformer, a low cost self oscillating flyback converter can be used to supply the auxiliary control circuitry.

7. RESULTS AND DISCUSSION

In this section, we will briefly discuss all the results achieved in this paper. We focus primarily on the need for a DC grid, which supplies direct DC power to appliances, thereby eliminating the need for an inverter, especially when power is generated from

solar panels. This approach increases the system's reliability [5]. In Section 3, we discussed the switching losses of FETs, and from *equations 3* and *equation 4*, it is evident that the conduction losses of the FET are lower when the supply is DC. This is further validated in section 5.4, in this test, the temperature of an IGBT of an induction stove was monitored, corresponding temperature rise is observed as shown in *figure 18*. The graph clearly shows that at 220 V, the temperature on the body (case) of the IGBT is lower with the DC input as compared to an AC input, indicating lower losses. The components required for implementing a DC grid are mentioned in the hardware results section. The battery charging and management system is specifically designed for this type of DC grid. Due to multiple tapings needed to achieve different voltage levels, a Battery Management System (BMS) is necessary to ensure the state of charge is maintained uniformly across all cells/batteries.

In Section 6, we discussed the modifications needed to convert certain electrical loads to Hybrid Electrical Loads (HEL). Heating loads, such as an iron box with a thermostat switch, experience terminal welding when DC is applied due to the absence of zero crossing. This results in unquenched arcing

across the terminals, as observed from the scope waveform shown in *figure 20*, which displays the current drawn by the iron box. The same issue can be seen in the hardware image shown in *figure 22*. By adding a capacitor across the thermostat switch, arcing was reduced, and the switch turned off without permanent arcing, as seen in *figure 21* and *figure 23*.

These slight modifications to electrical appliances enable the direct supply of DC power to the appliances. This study emphasizes that a local DC grid can be set up with a lower bill of materials (BOM), resulting in reduced costs and enhanced reliability [5]. Since most modern electrical appliances are inverter-based, they fall under the category of Hybrid Electrical Loads (HEL). In this paper, we have also explored methods to convert some non-HEL appliances into HEL appliances.

Table 4 shows the economic analysis of using AC and DC Grid and how DC grid has edge over AC. Since DC grid is having fewer system components its reliability increases and at the same time reducing the cost of the entire system. This table provides a clear comparison to highlight where cost savings and efficiency gains occur in a DC microgrid versus an AC microgrid.

Table 4. Economic Analysis of AC and DC Grid

Component/ Factor	AC Microgrid	DC Microgrid	Notes
Solar Panels	Same for both	Same for both	-
Inverter	High	None/Low	Cost of inverter eliminated in DC
Power Converters	Needed	Fewer Needed	DC needs fewer converters
Installation Cost	Moderate	Lower	Less complex wiring for DC
Maintenance (5-year period)	High	Lower	Fewer components to maintain
Operational Efficiency	Lower	Higher	DC minimizes conversion losses

7.1 Scalability of the Proposed DC Microgrid

The proposed DC microgrid, while designed for a single residential setup, can be effectively scaled to serve larger communities or neighbourhoods. Key considerations for scalability include efficient power flow management, where distributed energy resources (DERs) such as solar panels and battery storage are coordinated using smart energy management systems (EMS). Additionally, grid integration can be facilitated with hybrid AC-DC interfaces, allowing for seamless interaction with the main grid. A distributed control system is crucial in larger setups to manage power distribution autonomously at each node while maintaining overall system stability. Lastly, modular microgrids can be implemented, where smaller independent grids operate locally but interconnect for energy sharing, enhancing the system's reliability and resilience.

7.2 Control and Management of the DC Microgrid

As we transition towards standalone DC grids, expanding and interconnecting multiple DC grids is inherently simpler compared to AC systems, as synchronization issues like frequency and phase are eliminated. In DC grids, maintaining

consistent voltage levels is the primary requirement for interconnection. Utilizing a centralized control system can facilitate the expansion of a DC microgrid from a single residential setup to a larger community, such as a gated neighborhood. This centralized control enables efficient coordination of power flow, voltage regulation, and load management, ensuring stable and reliable operation as the grid scales.

8. CONCLUSION

Having a DC system with voltage level the same as the RMS voltage of the existing AC grid has been shown to be compatible for operation of HEL efficiently without additional power converters. This standardization of voltage will do away with the need to have power converters or special loads tailored for a non-compatible DC level. Mass produced appliances and loads will seamlessly work on the existing AC grids as well as the proposed DC level. The DC level was established with an integrated battery monitoring and charge equalization system, and having taps at different voltage levels for EV charging has been demonstrated. Minor modification in certain class of loads have been demonstrated for DC compatibility, and motor loads

with micro-inverters have the advantage of a better operational experience and can integrate into smart homes.

A consumer level DC Microgrid at the proposed voltage level coupled with a regulatory framework standardizing the voltage level, would incentivise energy efficient consumer appliances that are capable of hybrid operation. This would encourage the transition to efficient and reliable consumer level renewable energy based DC Microgrid with storage, and result in minimal disruption to the existing infrastructure, even with increased consumer loads and large scale EV penetration.

REFERENCES

[1] F. S. Al-Ismael, "DC microgrid planning, operation, and control: A comprehensive review," *IEEE Access*, vol. 9, 36154-36172, 2021.

[2] A. El-Shahat and S. Sumaiya, "DC-microgrid system design, control, and analysis," *Electronics*, vol. 8, no. 2, 2019.

[3] Kapustin, Nikita O and Dmitry A Grushevenko, 2020, "Long-term electric vehicles outlook and their potential impact on electric grid", *Energy Policy* 137, 111103.

[4] Madhu, MC, K Badari Narayana, and J Krishna Kishore, 2021, "Hybrid DC-AC homes with roof top solar power", *E3S Web of Conferences*. Vol. 239. *EDP Sciences*, 00017.

[5] Raghumanth, A and Joseph (2020), "A Minimally Disruptive DC Micro Grid for Hybrid Consumer Applications", *2020 IEEE International Conference on Power Systems Technology (POWERCON)*. IEEE, 1_6.

[6] Sabry, Ahmad H, Abidaoun H Shallal, Hayder Salim Hameed, and Pin Jern Ker (2020), "Compatibility of household appliances with DC microgrid for PV systems", *Heliyon* 6(12), e05699.

[7] Duijsen, Peter van, Johan Woudstra, and Diëgo Zuidervliet, 2019, "Requirements on Power Electronics for converting Kitchen Appliances from AC to DC", *2019 International Conference on the Domestic Use of Energy (DUE)*. IEEE, 190_197.

[8] Wang, Hongyu, TaoZhang, and BaohuiZhang (2019), "Selection of DC Voltage Level in household Hybrid AC/DC power supply system", *2019 IEEE 8th International Conference on Advanced Power System Automation and Protection (APAP)*. IEEE, 1527_1530.

[9] Mouli, Gautham Ram Chandra, Jos Schij_elen, Mike van den Heuvel, Menno Kardolus, and Pavol Bauer, 2018, "A 10 kW solar-powered bidirectional EV charger compatible with chademo and COMBO", *IEEE transactions on Power electronics* 34(2), 1082_1098.

[10] Prem, P, P Sivaraman, JS Sakthi Suriya Raj, M Jagabar Sathik, and Dhafer Almakhlis, 2020, "Fast charging converter and control algorithm for solar PV battery and electrical grid integrated electric vehicle charging station", *Automatika* 61(4), 614_625.

[11] Muhammad Anees, Taha Moaz, Sajid Hussain and Hassan Abbas Khan, Mashood Nasir, "Evaluation of system losses for 48 V and 380 V Solar Powered LVDC Microgrids", *2020 IEEE Power & Energy Society General Meeting (PESGM)*.

[12] Musavi, Fariborz, Gautam, Eberle, and Dunford (2013), "A simplified power loss calculation method for PFC boost topologies", *2013 IEEE Transportation Electri_cation Conference and Expo (ITEC)*. IEEE, 1_5.

[13] Park, Dong-Min, Seong-KyuKim, and Yeong-SeokSeo (2019), "S-mote: SMART home framework for common household appliances in IoT network", *Journal of Information Processing Systems* 15(2), 449_456.

[14] Shashank, Apurva, Vincent, Sivaraman, Balasundaram, Rajesh, and Ashokkumar (2021), "Power analysis of household appliances using IoT", *2021*

International Conference on System, Computation, Automation and Networking (ICSCAN). IEEE, 1_5.

[15] Shen, Lei, QimingCheng, Cheng, LinWei, and YujiaoWang (2020), "Hierarchical control of DC microgrid for photovoltaic EV charging station based on _ywheel and battery energy storage system", *Electric power systems research* 179, 106079.

[16] Biya, TS and Sindhu (2019), "Design and power management of solar powered electric vehicle charging station with energy storage system", *2019 3rd International conference on Electronics, Communication and Aerospace Technology (ICECA)*. IEEE, 815_820.

[17] Vikas, K Sankaraditya, B Raviteja Reddy, SG Abijith, and MR Sindhu, 2019, "Controller for charging electric vehicles at workplaces using solar energy", *2019 International Conference on Communication and Signal Processing (ICCSP)*. IEEE, 0862_0866.

[18] Khalid, Mohd Rizwan, Mohammad Saad Alam, Adil Sarwar, and MS Asghar (2019), "A Comprehensive review on electric vehicles charging infrastructures and their impacts on power-quality of the utility grid", *ETransportation* 1, 100006.

[19] Singh, Shakti, Prachi Chauhan, and Nirbhov Jap Singh, 2020, "Feasibility of grid-connected solar-wind hybrid system with electric vehicle charging station", *Journal of Modern Power Systems and Clean Energy* 9(2), 295_306.

[20] Verma, Anjeet, Bhim Singh, Ambrish Chandra, and Kamal Al-Haddad, 2020, "An implementation of solar PV array based multifunctional EV charger", *IEEE Transactions on Industry Applications* 56(4), 4166_4178.

[21] Ghosh, Aritra, 2020, "Possibilities and challenges for the inclusion of the electric vehicle (EV) to reduce the carbon footprint in the transport sector: A review", *Energies* 13(10), 2602.

[22] Rietmann, Nele, Beatrice Hügler, and Theo Lieven, 2020, "Forecasting the trajectory of electric vehicle sales and the consequences for worldwide CO2 emissions", *Journal of Cleaner Production* 261, 121038.

[23] Rajamani, Rajesh, and Willjuice Iruthayarajan (2022), "A PID control scheme with enhanced non-dominated sorting genetic algorithm applied to a non-inverting buck-boost converter", *Sadhana – Academy*

[24] Carlos Gomez-Aleixandre Angel Navarro-Rodriguez, Geber Villa, Cristian Blanco, Pablo Garcia, "Adaptive Droop Controller for a Hybrid 375 Vdc/48 Vdc/400 Vac AC/DC Microgrid", *IEEE Transactions on Industry Applications*, Vol. 58, No. 4, July/August 2022

[25] Himansu Sahoo, Santanu Kapat, Bhim Singh, "Small-Signal Modelling and Analysis of Converter Interactivity in 48 V DC Grid", *IEEE Transactions on Industry Applications*, Vol. 59, No. 5, September/October 2023.



© 2024 by the Raghumanth A and Rex Joseph
Submitted for possible open access publication
under the terms and conditions of the Creative
Commons Attribution (CC BY) license
(<http://creativecommons.org/licenses/by/4.0/>).